Available online at www.sciencedirect.com

ScienceDirect

Advances in Climate Change Research xxx (xxxx) xxx

www.keaipublishing.com/en/journals/accr/

Profound loss of microbial necromass carbon in permafrost thaw-subsidence in the central Tibetan Plateau

Wen-Ting ZHOU[a,b,c], Quan-Lian LI[b], Shi-Chang KANG[b,c], Xiao-Dong WU[a,b], Tian MA[d], Xiao-Bo WU[b], Xin XIONG[e], Tanuj SHUKLA[b], Maheswar RUPAKHETI[f], Dipesh RUPAKHETI[g], Da-He QIN[b,c], Xiu-Feng YIN[a,b,*]

[a] *Cryosphere Research Station on the Qinghai−Tibet Plateau, State Key Laboratory of Cryospheric Science, Northwest Institute of Eco-Environment and Resources, Chinese Academy of Sciences, Lanzhou 730000, China*

[b] *Key Laboratory of Cryospheric Science and Frozen Soil Engineering, Northwest Institute of Eco-Environment and Resources, Chinese Academy of Sciences, Lanzhou 730000, China*

[c] *University of Chinese Academy of Sciences, Beijing 100049, China*

[d] *State Key Laboratory of Herbage Improvement and Grassland Agro-ecosystems, and College of Pastoral Agriculture Science and Technology, Lanzhou University, Lanzhou 730020, China*

[e] *Lushan Botanical Garden, Chinese Academy of Sciences, Jiujiang 332900, China*

[f] *Research Institute for Sustainability-Helmholtz Centre Potsdam, Potsdam 14467, Germany*

[g] *Jiangsu Key Laboratory of Atmospheric Environment Monitoring and Pollution Control, Collaborative Innovation Center of Atmospheric Environment and Equipment Technology, School of Environmental Science and Engineering, Nanjing University of Information Science and Technology, Nanjing 210044, China*

Received 18 January 2024; revised 26 April 2024; accepted 2 July 2024

Abstract

Climate warming is causing rapid permafrost degradation, including thaw-induced subsidence, potentially resulting in heightened carbon release. Nevertheless, our understanding of the levels and variations of carbon components in permafrost, particularly during the degradation process, remains limited. The uncertainties arising from this process lead to inaccurate assessments of the climate effects during permafrost degradation. With vast expanses of permafrost in the Tibetan Plateau, there is limited research available on SOC components, particularly in the central Tibetan Plateau. Given remarkable variations in hydrothermal conditions across different areas of the Tibetan Plateau, the existing limited studies make it challenging to assess the overall SOC components in the permafrost across the Tibetan Plateau and simulate their future changes. In this study, we examined the properties of soil organic carbon (SOC) and microbial necromass carbon (MicrobialNC) in a representative permafrost thaw-subsidence area at the southern edge of continuous permafrost in the central Tibetan Plateau. The results indicate that prior to the thaw-subsidence, the permafrost had a SOC content of 72.68 ± 18.53 mg g^{-1}, with MicrobialNC accounting for 49.6%. The thaw-subsidence of permafrost led to a 56.4% reduction in SOC, with MicrobialNC accounting for 70.0% of the lost SOC. MicrobialNC constitutes the primary component of permafrost SOC, and it is the main component that is lost during thaw-subsidence formation. Changes in MicrobialNC are primarily correlated with factors pH, plant input, and microbial properties. The present study holds crucial implications for both the ecological and biogeochemical processes associated with carbon release from permafrost, and it furnishes essential data necessary for modeling the global response of permafrost to climate warming. Based on this study and previous research, permafrost thawing in the Tibetan Plateau causes substantial loss of SOC. However, there's remarkable heterogeneity in SOC component changes across different regions, warranting further in-depth investigation.

Keywords: Tibetan Plateau; Thaw-subsidence; Soil organic carbon; Microbial necromass carbon; Amino sugars

* Corresponding author. Key Laboratory of Cryospheric Science and Frozen Soil Engineering, Northwest Institute of Eco-Environment and Resources, Chinese Academy of Sciences, Lanzhou 730000, China.

E-mail address: yinxf@lzb.ac.cn (YIN X.-F.).

Peer review under responsibility of National Climate Centre (China Meteorological Administration).

https://doi.org/10.1016/j.accre.2024.07.002

Please cite this article as: ZHOU, W.-T., et al., Profound loss of microbial necromass carbon in permafrost thaw-subsidence in the central Tibetan Plateau, Advances in Climate Change Research, https://doi.org/10.1016/j.accre.2024.07.002

1. Introduction

Global surface temperature increased by 1.1 °C between 2011 and 2020, compared to 1850−1900 (IPCC, 2021). The increase in surface temperature has resulted in the thawing of permafrost soils, which are typically frozen year-round (Brown and Romanovsky, 2008). However, it is still unclear how much the effects of warming climates will impact the degradation of permafrost soils. Permafrost stores around 1.5 Mt of organic carbon in the Northern Hemisphere, twice of total amount of carbon present in the atmosphere (Lindgren et al., 2018). The rapid degradation of permafrost results in the formation of thermokarst landforms and leads to the release of carbon, which accelerates global warming then further exacerbates permafrost degradation (Schuur and Abbott, 2011; Natali et al., 2021). Therefore, the carbon release resulting from permafrost degradation plays a positive feedback role in the process of global warming (Matthews et al., 2009).

Carbon present in permafrost soils consists of different carbon components (*e.g.*, microbial necromass carbon and plant-derived carbon), each with distinct properties (Chang et al., 2021; Zhou et al., 2023). These components exhibit variations in loss rates during the process of permafrost carbon loss (Zhou et al., 2023). Assessing the proportions of carbon from different components in permafrost, as well as understanding their characteristics during rapid degradation, is of crucial importance for accurately predicting future changes in permafrost carbon (Mu et al., 2020; Miner et al., 2022). Microbial necromass carbon, due to their high proportion of SOC (soil organic carbon), serve not only as remarkable soil carbon reservoirs but also exert a substantial influence on soil carbon stock dynamics (Wang et al., 2021; Cao et al., 2023).

The Tibetan Plateau is the largest region of permafrost distribution (1.06 million km^2 out of 2.50 million km^2) at mid-low latitudes over the world (Zou et al., 2017) and is highly sensitive to climate change. The SOC pool in upper 2-m permafrost in the Tibetan Plateau is estimated as big as 17.1−19.0 Pg (Mu et al., 2015, 2020). Permafrost degradation in this region is occurring at a rapid pace (Luo et al., 2019) and thaw-subsidence is one of the important forms of rapid permafrost degradation in the Tibetan Plateau, leading to the substantial release of soil organic carbon (Chen et al., 2016; Wang et al., 2020; Zhou et al., 2023).

The permafrost regions of the Tibetan Plateau cover a vast area, exhibiting remarkable variations in soil moisture and thermal conditions across different regions (Wang et al., 2012; Zhao et al., 2021). This is potentially to result in different structures of SOC components in permafrost in various regions, and to undergo distinct components changes after permafrost degradation. Currently, research on the SOC components in the Tibetan Plateau is primarily focused on its northern region (Zhou et al., 2023). We still lack in systematic research on the loss of carbon components, such as microbial necromass carbon, during the rapid degradation of permafrost, especially in the central and southern Tibetan Plateau. Due to the lack of relevant research, there is noticeable uncertainty in understanding the mechanisms and predictions of carbon release from rapid permafrost degradation. This study focuses on the loss of SOC and microbial necromass carbon in a typical permafrost thaw-subsidence at the southern edge of continuous permafrost in the central Tibetan Plateau. It quantifies the contribution of microbial necromass carbon to SOC loss and elucidates the relationship between microbial necromass carbon and environmental factors. Furthermore, this study compares the variations in SOC components and their changes during the rapid degradation between the northern and southern regions of continuous permafrost distribution in the Tibetan Plateau. The results of this study can provide new perspectives and foundational data for better predicting the changes in permafrost carbon trends in the context of global change.

2. Materials and methods

2.1. Study area

A typical permafrost thaw-subsidence (91.77°E, 32.01°N, and 4672 m a.s.l.) at the southern edge of continuous permafrost over the Tibetan Plateau (Zou et al., 2017) at Amdo was selected as the study area (Fig. 1). The ice-rich permafrost, with average active layer thickness of ~2.5 m, in this region led to massive thaw-subsidence (Wu et al., 2018). The annual precipitation in this area is ~350 mm (Wu et al., 2018). The primary soil category consists of colluvial deposits. The land cover corresponds to alpine meadow. The sampling site exhibits a slope of 1° and faces the aspect of 270°.

2.2. Experimental design and soil sampling

We conducted our experiment in August 2021, during which soil samples were systematically collected. The thaw-subsidence selected is consists of two adjacent units (subsidence S and subsidence N in Fig. 1). Subsidence S is an oval terrain with a major axis of 13 m and a minor axis of 9 m. Subsidence N is a striped terrain measuring 80 m in length and 6 m in width. The thaw-subsidence is actively developing in a depth of approximately 1 m. Similar thaw-subsidences are widely distributed in this area.

The sampling process was conducted in three sampling stages: control, collapsing, and subsided. The control stage refers to the soil that has not been affected by permafrost thaw-subsidence occurs. The collapsing stage represents the location where thaw-subsidence are currently occurring, and it is still situated on the most recently formed vertical profile of the original soil. The subsided stage refers to the completed thaw-subsidence, where the entire thaw-subsidence mass has detached from the original soil and is currently situated below the original soil level. The sample collection includes two areas, subsidence S (subsided-S, collapsing-S, and control-S) and subsidence N (collapsing-N1, subsided-N, collapsing-N2, and control-N), conducted from south to north (Fig. 1). In

Please cite this article as: ZHOU, W.-T., et al., Profound loss of microbial necromass carbon in permafrost thaw-subsidence in the central Tibetan Plateau, Advances in Climate Change Research, https://doi.org/10.1016/j.accre.2024.07.002

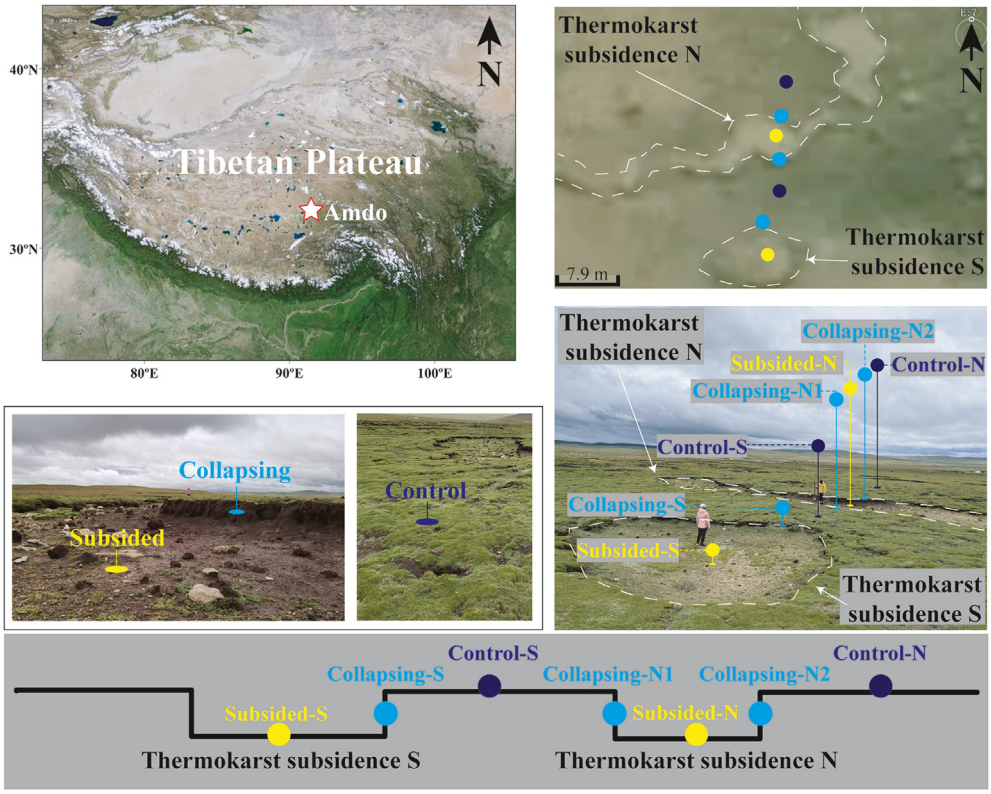

Fig. 1. Study area and sampling sites at Amdo in the central Tibetan Plateau (Permafrost distribution was obtained from Zou et al. (2017)).

each thaw-subsidence, sampling sites in the control stage were situated approximately 5 m away from the corresponding sites in the collapsing stage, positioned at the natural profiles along the periphery of the subsidence unit. Sampling sites in the subsided stage were located centrally within the subsidence unit, approximately 3−5 m away from the corresponding collapsing stage sampling sites. In each stage, three parallel pits were excavated within 1 m × 1 m plots. Soil samples were collected from 20 cm × 20 cm areas at depths of 0−10, 10−20, and 20−40 cm for each pit, along with measurements of aboveground and belowground biomass.

2.3. Soil physical and chemical parameters, microbial community composition and microbial biomass

We tested following physical and chemical parameters: SOC, total nitrogen (TN), soil texture, soil moisture (SM), bulk density (BD), pH, aboveground biomass (AGB), belowground biomass (BGB), dithionite-extractable iron (Fe_d), and dithionite-extractable aluminum (Al_d). After field sampling, roots in all samples were filtered out by passing through a 2-mm mesh before analysis to measure belowground biomass. After removal of inorganic carbon from samples we analysed total SOC and nitrogen through elemental analyzer instrument (Vario Isotope Select, Elementar, Germany) equipped with Thermal Conductivity Detector and the instrument precision <0.1% (external precision, 1σ). Furthermore, SOC stock (C stock), soil texture, soil moisture, pH, Fe_d, Al_d, AGB, BGB were measured according to the processes described in Zhou et al. (2023), Ma et al. (2018), and Mckeague et al. (1966). Each sample is tested three times in replicates for the above parameters as well as microbial community composition, microbial biomass, and amino sugars.

To assess both microbial biomass and microbial community composition, total PLFAs (phospholipid fatty acids) (Bossio and Scow, 1998; Frostegård and Bååth E, 1996) were examined. Total PLFAs were categorized into Gram-negative bacteria (G−), Gram-positive bacteria (G+), fungi, and unspecified PLFA through measurements (Zelles, 1999). The composition of the microbial community was evaluated using the ratios of fungal phospholipid fatty acids (F) to bacterial phospholipid fatty acids (B) and G−/G+. PLFAs were classified following the standard PLFA nomenclature (Guckert et al., 1985). Various peaks in the measurements were distinguished and attributed to G+, G− and fungi. The total PLFAs were calculated as the sum of all peaks identified in a given sample.

2.4. Analysis of amino sugars and calculation of microbial necromass carbon

The quantification of biomarkers was performed using internal standards on a gas chromatograph (Trace ITQ1100, Thermo Fisher Scientific, USA). Amino sugars pretreatment and heating scheme were carried out according to the processes described in Zhou et al. (2023) and Ma et al. (2018). Soil samples were hydrolyzed with 6 M HCl at 105 °C for 8 h. Myo-inositol (100 μg) was added as a surrogate standard and then filtered, followed by evaporation and re-dissolution in

Please cite this article as: ZHOU, W.-T., et al., Profound loss of microbial necromass carbon in permafrost thaw-subsidence in the central Tibetan Plateau, Advances in Climate Change Research, https://doi.org/10.1016/j.accre.2024.07.002

5 mL of MilliQ water with pH adjusted to 6.6−6.8 using 1 M potassium hydroxide. After centrifugation and freeze-drying, the supernatant was dissolved in methanol to separate amino sugars from salts. Derivatization involved heating the samples with a reagent at 75 °C for 30 min, followed by acetylation at 75−80 °C for 20 min. After removing excess reagents, the derivatives were dried under nitrogen for quantification. Quantification was achieved by comparing surrogate standards with compound loss during extraction procedures. External quantification standards were employed to normalize the response factor for individual amino sugars, including mannosamine (ManN), muramic acid (MurA), glucosamine (GluN) and galactosamine (GalN).

Amino sugars serve as reliable indicators for assessing the proportion of microbial necromass carbon within SOC (Li et al., 2020; Deng et al., 2022; Zhou et al., 2023). The determination of MicrobialNC (microbial necromass carbon, MNC) in this study involved the computation using amino sugars, employing the approach outlined in Liang et al. (2019) and Appuhn and Joergensen (2006). The cumulative MicrobialNC comprises fungal necromass carbon (FungalNC) and bacterial necromass carbon (BacterialNC). FungalNC is calculated as (GluN/179.17 − 2 × MurA/251.23) × 179.17 × 9, while BacterialNC is determined by MurA multiplied by the factor *n*. To control errors in amino sugar analysis (Whalen et al., 2022), we calculated a bacterial conversion factor (*n*) individually for each sample (Appuhn and Joergensen, 2006; Cao et al., 2023). The bacterial conversion factor varies from 45 to 52 (with an average of 49), and each sample utilizes its uniquely calculated conversion factor.

2.5. Statistical analyses

We explored the distinctions in SOC, amino sugars, and various soil physicochemical characteristics across different stages using one-way ANOVAs coupled with the least significant difference test. The investigation of connections between parameters involved the use of the Pearson correlation coefficient with a two-tailed test. Statistical significance was determined at a threshold of 0.05. The statistical analyses was performed using IBM SPSS Statistics 25.

Utilizing SmartPLS 3, we employed partial least squares path modeling (PLS-PM) to explore the impact of soil variables on MicrobialNC in permafrost thaw-subsidence. The model path underwent 5000 bootstraps for the validation of path coefficients and estimates of explained variability (R^2). Goodness-of-fit (GOF) statistics were employed to assess the models. For PLS-PM calculations, each parameter encompasses 63 data points.

3. Results

3.1. Thaw-subsidence induced soil environment variation

The collapse of soil mass along the boundaries of thaw-subsidence results in the exposure of soil profiles, leading to structural deformation in these soils. Environmental factors are varied during the formation of thaw-subsidence (Table 1). The soils in the subsided stage have the lowest TN concentration, SOC/TN, soil moisture, aboveground biomass, and belowground biomass, but with the highest bulk density and pH.

The calculated TN values indicate an approximately 28.5% decline from the control stage to the subsided stage. Additionally, there is a remarkable reduction in SOC/TN, dropping from 15.39 ± 3.76 in the control stage to 10.65 ± 6.01 in the subsided stage. Similarly, SM content has notably decreased from 55.11% ± 18.74% in the control stage to 25.72% ± 6.70% in the subsided stage. Contrary to soil moisture, bulk density has increased during the formation of thaw-subsidence and found to be 82.8% higher from the subsided stage than the control stage. The subsided and the collapsing areas exhibited significantly lower soil moisture content as well as higher bulk density, which could be attributed to the exposure of natural soil profiles and the deformation of soil structure. This, in turn, contributed to increased evaporation and improved drainage conditions (Jensen et al., 2014). We have also observed an increase in pH values from 7.37 in the control stage to 7.88 in the subsided stage. The aboveground biomass and belowground biomass are lower in the subsided stage than in the other two stages.

The stage-mean Fe_d decreases sequentially from the control stage to the collapsing stage and further to the subsided stage. Interestingly, Fe_d exhibits divergent depth-related trends. It increases from the control stage to the subsided stage in the 0−10 cm layer but decreases in the 20−40 cm layer. On the other hand, Al_d shows a consistent increase from the control stage to the subsided stage. The overall mean percentages of clay, silt, and sand are 8.39% ± 2.83%, 33.7% ± 13.83%, and 58.54% ± 15.65%, respectively, indicating intricate variations across different depths.

3.2. Variations of soil microbial characteristics

The results from total PLFAs show an increase from the control stage (0.62 ± 0.19 mg g^{-1} SOC) to the collapsing stage (0.78 ± 0.28 mg g^{-1} SOC), followed by a decrease in the subsided stage (0.66 ± 0.35 mg g^{-1} SOC) (Fig. 2). Total PLFAs in the 0−10 cm depth are found to be higher than those in the 10−20 and 20−40 cm depths for all three stages. The overall mean concentration of bacterial PLFAs is more than four times higher than that of fungal PLFAs. Similar trends are observed in bacterial and fungal PLFAs with total PLFAs, with low concentrations of both observed in the subsided stage. The stage-mean of F/B varies between 0.17 and 0.19 in the three stages and is higher in the surface layer (0−10 cm) than in the other two depths (10−20 and 20−40 cm). G−/G+ in the 0−10 cm layer increases from the control stage (0.70 ± 0.06) to the collapsing stage (0.79 ± 0.06), and then further to the subsided stage (0.89 ± 0.03). In the 20−40 cm depth, G−/G+ in the subsided stage is much lower than in the other two stages, with a smaller variation ranging from 0.75 to 0.80.

By comparing the results from present study of variation in total PLFAs, bacterial PLFAs, and fungal PLFAs, F/B, and

Please cite this article as: ZHOU, W.-T., et al., Profound loss of microbial necromass carbon in permafrost thaw-subsidence in the central Tibetan Plateau, Advances in Climate Change Research, https://doi.org/10.1016/j.accre.2024.07.002

Table 1
Mean concentrations of parameters at different depths (0−10, 10−20, and 20−40 cm) during different stages (control, collapsing, and subsided) of permafrost thaw-subsidence.

Parameter	Control				Collapsing				Subsided				Overall
	Mean	0−10 cm	10−20 cm	20−40 cm	Mean	0−10 cm	10−20 cm	20−40 cm	Mean	0−10 cm	10−20 cm	20−40 cm	Mean
SOC (mg g^{-1})	72.68	61.35	65.98	90.72	62.06	52.63	58.26	75.28	31.67	32.06	34.39	28.55	56.41
SOC Stock (kg m^{-2})	4.14	3.21	2.66	6.56	3.95	2.94	2.09	6.80	3.24	2.52	2.60	4.60	3.78
Amino sugars (mg g^{-1} SOC)	74.72	85.55	80.59	58.01	65.61	80.00	66.25	50.59	39.36	47.57	40.70	29.79	60.71
Fungal NC (% SOC)	42.27	48.98	46.34	31.49	37.30	46.55	38.27	27.08	19.49	26.40	18.46	13.60	33.63
Bacterial NC (% SOC)	7.33	8.81	7.96	5.23	6.01	7.72	5.34	4.96	3.75	5.07	3.14	3.05	5.74
MNC (% SOC)	49.61	57.79	54.30	36.73	43.31	54.27	43.61	32.04	23.24	31.47	21.60	16.64	39.37
TN (mg g^{-1})	4.92	4.34	4.37	6.06	5.56	5.08	5.49	6.10	3.52	3.89	3.59	3.08	4.79
SOC/TN	15.39	14.58	15.77	15.80	11.15	10.42	10.62	12.42	10.65	9.85	11.19	10.90	12.22
Soil moisture (%)	55.11	35.48	63.00	66.84	44.00	33.24	59.04	39.71	25.72	20.12	29.89	27.15	41.95
Bulk density (kg m^{-3})	429.84	528.61	401.63	359.27	462.13	557.76	359.95	468.68	785.67	785.73	755.05	816.24	545.34
pH	7.37	7.35	7.22	7.54	7.67	7.55	7.64	7.83	7.88	7.89	7.81	7.95	7.65
Bacterial PLFAs (ug g^{-1} SOC)	418.83	486.77	432.61	337.11	534.34	675.13	576.37	351.52	451.13	696.81	350.79	305.79	477.56
Fungal PLFAs (ug g^{-1} SOC)	73.76	93.27	76.04	51.98	102.59	137.21	112.34	58.21	83.26	149.32	56.50	43.94	88.83
F/B	0.17	0.19	0.18	0.15	0.19	0.20	0.19	0.17	0.18	0.22	0.17	0.15	0.18
G−/G +	0.75	0.70	0.75	0.79	0.81	0.79	0.80	0.84	0.76	0.89	0.75	0.63	0.78
Unspecified PLFAs (ug g^{-1} SOC)	127.56	153.21	132.32	97.16	144.76	180.16	154.20	99.90	127.36	178.39	100.69	103.00	134.87
Total PLFAs (mg g^{-1} SOC)	0.62	0.73	0.64	0.49	0.78	0.99	0.84	0.51	0.66	1.02	0.51	0.45	0.70
Fe_d (%)	0.55	0.49	0.52	0.66	0.54	0.53	0.52	0.58	0.52	0.54	0.50	0.53	0.54
Al_d (%)	0.10	0.08	0.09	0.13	0.09	0.09	0.09	0.10	0.12	0.10	0.12	0.12	0.10
Clay (%)	9.13	5.43	10.77	11.18	8.76	7.03	8.05	11.20	7.10	6.74	8.42	6.16	8.39
Silt (%)	28.76	14.14	27.63	44.52	34.47	27.32	33.59	42.51	35.29	31.16	47.42	27.29	33.07
Sand (%)	62.11	80.43	61.60	44.30	56.77	65.65	58.37	46.30	57.61	62.10	44.17	66.56	58.54
Clay + silt (%)	37.89	19.57	38.40	55.70	43.23	34.35	41.63	53.71	42.39	37.90	55.83	33.44	41.46
Aboveground biomass (kg m^{-2})	1.34	1.34	1.34	1.34	1.23	1.23	1.23	1.23	0.46	0.46	0.46	0.46	1.04
Belowground biomass (kg m^{-2})	5.73	5.73	5.73	5.73	5.37	5.37	5.37	5.37	1.06	1.06	1.06	1.06	4.24

G−/G+ is found to be different from the other studies conducted in the northeastern Tibetan Plateau (Chen et al., 2018; Mao et al., 2019; Zhou et al., 2023). We hypothesized that variations in permafrost thermokarst landforms across different locations may result in distinct alterations in both microbial community composition and microbial biomass, potentially influenced by specific local environmental factors.

3.3. Dramatic SOC loss

The mean SOC concentration of two permafrost thaw-subsidences (S and N) decreases from the control stage (72.68 ± 18.53 mg g^{-1}) to the collapsing stage (62.06 ± 15.91 mg g^{-1}) and then to the subsided stage (31.67 ± 8.15 mg g^{-1}) (Fig. 3 and Table 1), showing a 56.4% of SOC decrease from the control stage to subsided stage. Mean SOC concentration is higher in 20−40 cm in the control and the collapsing stage than 0−10 and 10−20 cm. While in the subsided stage, mean SOC concentrations in all depth are low and in similar levels (28.55−34.39 mg g^{-1}). The largest loss of SOC from the control stage to subsided stage is in 20−40 cm with a rate of 68.5% (Table 1). The dramatic loss of SOC is also observed in 0−10 cm (47.7%) and 10−20 cm (47.9%) from the control stage to subsided stage (Fig. 3 and Table 1).

The SOC losing rate is comparable with the results from the northeastern Tibetan Plateau (Zhou et al., 2023), indicating the dramatic carbon loss from permafrost over the Tibetan Plateau during the formation of thaw-subsidence. Mostly based on SOC and bulk density, mean SOC stock in subsided stages is lower than the collapsing and the control stages showing a 21.7% decrease of SOC stocks from the control stage to the subsided stage (Table 1 and Fig. A1). The significant loss of SOC stock caused by thaw-subsidence differs from other ecosystems, such as forests, grasslands, and croplands, which generally witnessed remarkable increase or neutral change under global warming in SOC stock over recent decades. On a global scale, the mean annual SOC stock increase rate of these ecosystems amounts to 1.9‰ (Chen et al., 2015).

3.4. Contribution of microbial necromass carbon in SOC loss

The overall mean concentration of amino sugars in thaw-subsidence is 60.71 ± 24.21 mg g^{-1} SOC (Table 1). Amino

Please cite this article as: ZHOU, W.-T., et al., Profound loss of microbial necromass carbon in permafrost thaw-subsidence in the central Tibetan Plateau, Advances in Climate Change Research, https://doi.org/10.1016/j.accre.2024.07.002

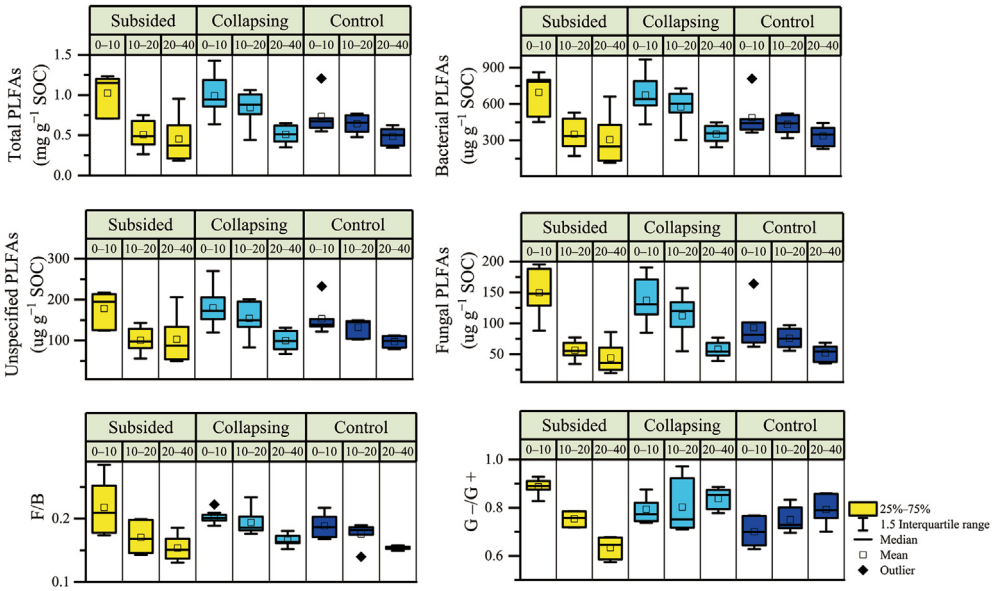

Fig. 2. Changes in total PLFAs, bacterial PLFAs, fungal PLFAs, unspecified PLFA, F/B, and G−/G+ at different depths (0−10, 10−20, and 20−40 cm) during different stages (control, collapsing, and subsided) of permafrost thaw-subsidence.

sugars concentrations in 0−10 cm (72.32 ± 25.39 mg g^{-1} SOC) in three stages are higher than those in 10−20 cm (63.05 ± 22.23 mg g^{-1} SOC) and 20−40 cm (46.77 ± 18.07 mg g^{-1} SOC) (Table 1). During the formation of thaw-subsidence, stage-mean concentration of amino sugars significantly decreases from the control stage (74.72 ± 24.03 mg g^{-1} SOC) to the collapsing stage (65.61 ± 19.58 mg g^{-1} SOC) then to the subsided stage (39.36 ± 15.65 mg g^{-1} SOC) (Fig. 4), showing a 47.3% decrease from the control stage to the subsided stage. Dramatic loss of amino sugars is observed from the control stage to the subsided stage in each depth (0−10 cm: 44.4%; 10−20 cm: 49.5%; 20−40 cm: 48.6%). When looking at the absolute content of amino sugars in the soil, the decline caused by thaw-subsidence is more pronounced, leading to significant decrease from the control stage (5.09 ± 0.93 mg g^{-1} soil) to the collapsing stage (3.99 ± 1.24 mg g^{-1} soil) then to the subsided stage (1.23 ± 0.64 mg g^{-1} soil) showing a 75.8% off of absolute content of amino sugars in the soil from the control stage to the subsided stage.

Compared with amino sugar concentrations in previous studies (Cao et al., 2023), the amino sugar before thaw-subsidence formation (the control stage: 5.24 ± 1.18 mg g^{-1}, concentration is transferred into mg g^{-1} to compare with the results from other studies) is much larger than the highest mean concentration (temperate forest: 3.76 mg g^{-1}) in other ecosystems (temperate forest > boreal forest > wetland > tundra > subtropical forest > temperate grassland > subtropical grassland > tropical forest > tropical grassland > shrubland > cropland > bareland > desert). This indicates that amino sugar has a significantly high proportion in the permafrost, and it is very likely to dominate the variation of permafrost SOC. After thaw-subsidence occurs, the amino sugar content in permafrost at the subsided stage (0.86 ± 0.53 mg g^{-1}) surpasses only the minimum value observed in other ecosystems (0.24 mg g^{-1} in desert) (Cao et al., 2023). This indicates that the amino sugar concentration undergoes a significant decrease during the thaw-subsidence process in permafrost, and the magnitude of this reduction exceeds the gap observed among different ecosystems.

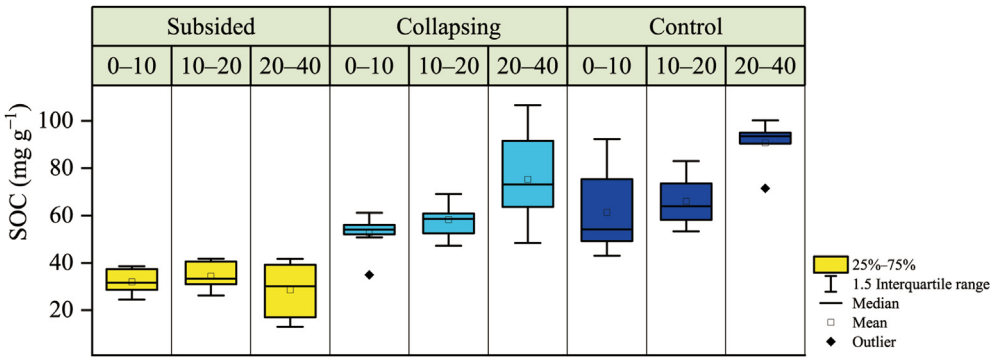

Fig. 3. Changes in soil organic carbon (SOC) at different depths (0−10, 10−20, and 20−40 cm) during different stages (control, collapsing, and subsided) of permafrost thaw-subsidence.

Please cite this article as: ZHOU, W.-T., et al., Profound loss of microbial necromass carbon in permafrost thaw-subsidence in the central Tibetan Plateau, Advances in Climate Change Research, https://doi.org/10.1016/j.accre.2024.07.002

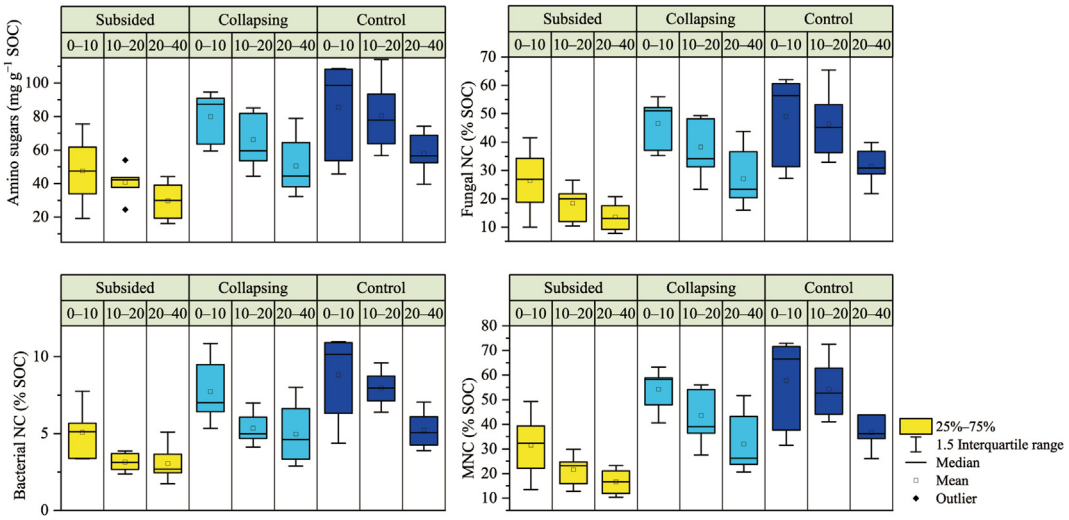

Fig. 4. Changes in amino sugars, microbial necromass carbon (MNC), fungal necromass carbon (FungalNC), and bacterial necromass carbon (BacterialNC) at different depths (0−10, 10−20, and 20−40 cm) during different stages (control, collapsing, and subsided) of permafrost thaw-subsidence.

MicrobialNC dominates the loss of SOC, accounting for 70.0% of the total lost SOC (from the control stage to the subsided stage, which amounts to 41.01 mg g^{-1}) during the formation of thaw-subsidence, which is much more than contributions from other components. The overall mean MicrobialNC in thaw-subsidence is 39.37% ± 17.05% SOC, showing a decrease in the following order: the control stage (49.61% ± 15.84% SOC) > the collapsing stage (43.31% ± 13.78% SOC) > the subsided stage (23.24% ± 10.37% SOC) (Fig. 4). The decrease rate of stage-mean MicrobialNC from the control stage to the subsided stage is 53.2%. Compared to previous studies (Cao et al., 2023), the contribution of MicrobialNC to SOC prior to the formation of thaw-subsidence (the control stage: 49.61%) is higher than in the majority of ecosystems and it is comparable to the highest levels observed in tundra (53.98%) and temperate grassland (53.23%). However, following the occurrence of subsidence, the contribution of MicrobialNC to SOC (the subsided stage: 23.24%) is lower even than the lowest recorded contribution across all ecosystems (wetland: 29.48%) (Cao et al., 2023). This highlights a substantial loss of MicrobialNC resulting from permafrost thaw-subsidence.

The overall mean FungalNC (24.49% ± 10.66% SOC) is more dominant than BacterialNC (4.49% ± 1.76% SOC) (Fig. 4). There could be several reasons for higher proportion of FungalNC than BacterialNC. Initially, fungi excel in nutrient acquisition as they can efficiently utilize recalcitrant compounds and those with a high C/N ratio for synthesizing their biomass, resulting in fungal biomass being three to four times greater than that of bacteria (Li et al., 2015; Wang et al., 2021). Moreover, fungal tissue has a higher capacity to store carbon compared to bacteria tissue when consuming the same amount of nitrogen (Sylvia et al., 2005; Bahram et al., 2018) and the presence of melanin in fungal filaments contributes to the higher stability of fungal residue compared to bacterial residue, as melanin inhibits the decomposition of organic carbon (Guggenberger et al., 1999). Similar decrease from the control stage to collapsing/subsided stage are shown in FungalNC, and BacterialNC in all three depths as well as MicrobialNC (Fig. 4).

3.5. Correlation of environmental parameters with MicrobialNC and PLS-PM results

Soil and microbial properties are the major factors influencing the variation of MicrobialNC (Wang et al., 2021; Cao et al., 2023). Based on the results of correlation coefficient and linear fit statistics (Figs. A2 and A3), MicrobialNC is correlated with soil moisture, bulk density, pH, Al_d, Silt, Sand, Clay + Silt, aboveground biomass, belowground biomass, total PLFAs, bacterial PLFAs, fungal PLFAs, unspecified PLFAs, and F/B Among all pentameters, MicrobialNC is positively correlated with aboveground biomass ($r = 0.51$, $p < 0.05$) and belowground biomass ($r = 0.52$, $p < 0.05$), while negatively correlated with pH ($r = -0.68$, $p < 0.05$). Besides, MicrobialNC is significantly positively correlated with the microbial characteristics (total PLFAs, bacterial PLFAs, fungal PLFAs, unspecified PLFAs, and F/B). PLS-PM results (Fig. 5) visualized the impacts from various parameters to the variation of MicrobialNC. It is found that permafrost thaw-subsidence exerts a significant impact on the variation of MicrobialNC (60% of the variation of MicrobialNC can be explained by thaw-subsidence formation) (Fig. 5). During the development of permafrost thaw-subsidence, pH (−0.54, $p < 0.05$), plant input (aboveground biomass and belowground biomass, 0.23, $p < 0.05$), clay (−0.18, $p < 0.05$), and microbial properties (0.24, $p > 0.05$) are the major influencing factors to MicrobialNC.

4. Discussion

The negative effects of pH on MicrobialNC can be attributed to its direct impacts on plant biome and soil substrate availability (Wang et al., 2021). The elevated pH levels

Please cite this article as: ZHOU, W.-T., et al., Profound loss of microbial necromass carbon in permafrost thaw-subsidence in the central Tibetan Plateau, Advances in Climate Change Research, https://doi.org/10.1016/j.accre.2024.07.002

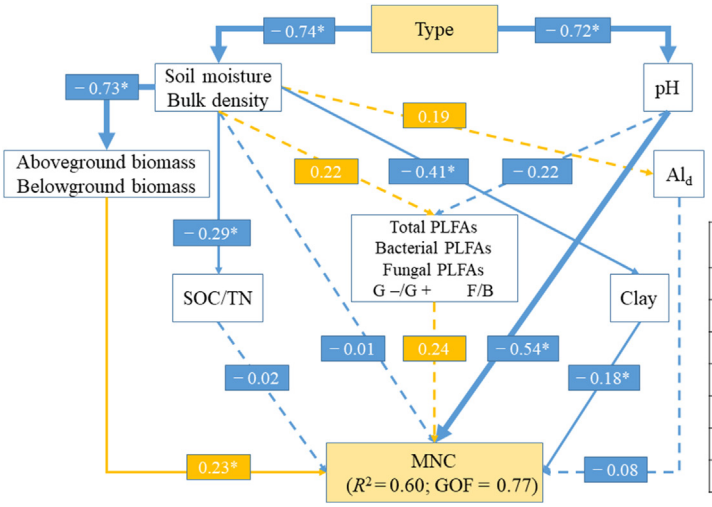

	Standardized total effect on MNC
pH	− 0.54*
AGB, BGB	0.23*
Clay	− 0.18*
Microbial properties	0.24
Al_d	− 0.08
SM, BD	− 0.01
SOC/TN	− 0.02

Fig. 5. Partial least squares path modeling (PLS-PM) showing the effects of permafrost thaw-subsidence on microbial necromass carbon (MNC), and standardized total effects of soil environmental variables derived from the PLS-PM (Numbers adjoining the arrows indicate standardized path coefficients, and the arrow width is proportional to the strength of the association. Orange Blue arrows represent positive/negative relationships. The solid/dashed arrows represent significant/non-significant relationships (*$p < 0.05$). R^2 values indicate the variance of variables accounted for by the model. Models were evaluated using the goodness of fit (GOF) statistics. SOC, soil organic carbon; TN, total nitrogen; AGB, aboveground biomass; BGB, belowground biomass; Al_d, dithionite-extractable aluminum; SM, soil moisture; and BD, bulk density. Type refers to the three stages of permafrost thaw-subsidence: control stage, collapsing stage, and subsided stage).

following thaw-subsidence events might contribute to increased microbial carbon use efficiency (Jones et al., 2019). Moreover, the breakdown of fungal necromass rises in correlation with soil pH (Hu et al., 2020). As thaw-subsidence occurs, soil moisture decreases, pH increases, improving soil structure permeability, and enhancing microbial decomposition intensity, potentially resulting in a decrease in MicrobialNC.

Plant input (AGB and BGB) exhibits a significant positive effect on MicrobialNC as root exudates and litter from plants serve as a source of energy, supporting soil microbial activities (He et al., 2022; Neher, 2010). After thaw-subsidence occurs, the decreased AGB and BGB limits the energy available for microbial growth and necromass accumulation, contributing to the decrease of MicrobialNC, surpassing the effect that more nutrients can be utilized by microorganisms with fewer plants competition.

A positive correlation is observed between microbial properties and MicrobialNC, potentially attributable to the ability of living microbes to recycle nutrients from degraded microbial residues. The unutilized portions of these residues accumulate in the soil as microbial residue (Gupta et al., 2017). With the occurrence of thaw-subsidence, the iterative process of microbial biomass and MicrobialNC is altered, disrupting the previous cyclic balance and probably leading to enhanced decomposition of microbial residue carbon, resulting to the decreased of MicrobialNC. Further research, including controlled experiments, is warranted to explore the causal relationship between changes in microbial biomass and microbial residue carbon at the species level.

The physicochemical protection, facilitated by soil minerals such as Fe_d/Al_d and clay fractions, may play a remarkable role in the stabilization of MicrobialNC. Fe_d/Al_d can facilitate the conversion of microbial residues into mineral-bound organic carbon (OC) through processes such as ligand exchange or co-precipitation (Hemingway et al., 2019; Kleber et al., 2015; Lützow et al., 2006). Furthermore, the ample specific surface area of clay soil materials can facilitate the development of microaggregates, consequently impeding the decomposition and utilization of MicrobialNC through physical occlusion (Lauer et al., 2011; Six et al., 2006). However, neither clay nor Fe_d/Al_d showed any positive impact on MicrobialNC and both of clay and Al_d showed a negative correlation with MicrobialNC. This could be due to the great spatial heterogenies in the soil environments in permafrost thaw-subsidence among the microfeatures. Some mechanisms during the thaw-subsidence process have a greater impact beyond physicochemical protection and merit further investigation.

The Tibetan Plateau permafrost covers a vast area, exhibiting significant variations in soil moisture and thermal conditions across different regions. Based on studies of thaw slump at Eboling in the northern Tibetan Plateau (Zhou et al., 2023) and thaw-subsidence at Amdo in the central Tibetan Plateau in this study (Eboling and Amdo are located respectively at the northern and southern boundaries of the continuous permafrost distribution on the Tibetan Plateau), we found that both thaw slump and thaw-subsidence result in significant losses of SOC in permafrost regions, amounting to 61.4% in the northern Tibetan Plateau and 56.4% in the central Tibetan Plateau from the control stage to the subsided/exposed stage (Fig. 6). In Zhou et al. (2023), the SOC content before permafrost degradation was higher than in this study. Although the SOC content in Zhou et al. (2023) after thaw-subsidence remains higher, the decrease in SOC content was slightly greater than the results of this study. In the aforementioned

Please cite this article as: ZHOU, W.-T., et al., Profound loss of microbial necromass carbon in permafrost thaw-subsidence in the central Tibetan Plateau, Advances in Climate Change Research, https://doi.org/10.1016/j.accre.2024.07.002

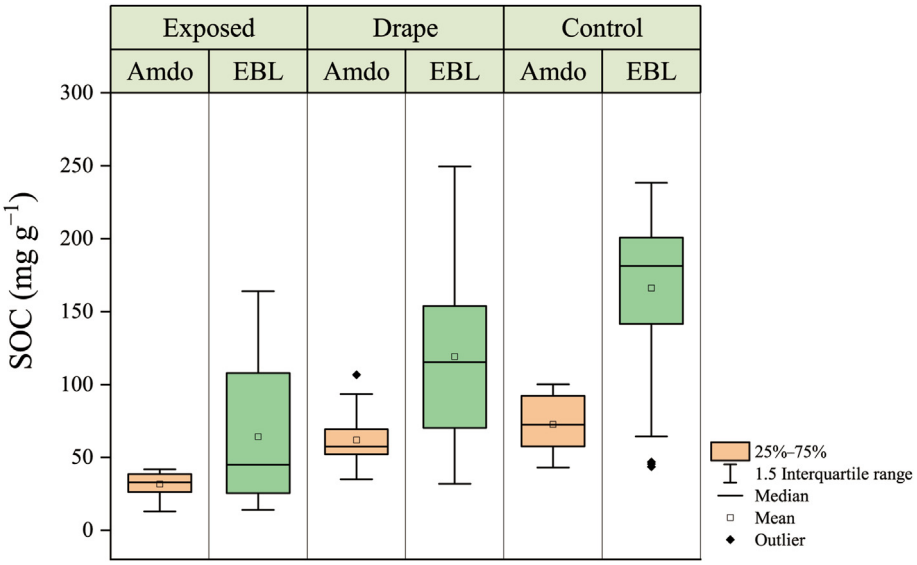

Fig. 6. Changes in soil organic carbon (SOC) at different sites in the central Tibetan Plateau (Amdo) and northern Tibetan Plateau (EBL, Zhou et al. (2023)) during different stages (control, collapsing, and subsided) of permafrost thaw-subsidence.

studies, the decline in SOC triggered by both thaw slumps and thaw-subsidence was primarily driven by the rapid decrease in MicrobialNC (Fig. 7). Furthermore, after rapid permafrost degradation, the MicrobialNC at the subsided/exposed stage was at a relatively similar level in both studies. While, previous studies on permafrost thaw revealed a remarkable decrease in SOC occurring within a decade after permafrost thaw in Shaliuhe in the Tibetan Plateau (Liu et al., 2022), consistent with the findings of this study and Zhou et al. (2023). However, Liu et al. (2022) found that the proportion of MicrobialNC experienced a remarkable increase within a decade after permafrost thaw, which is sharply contrary to the rapid decline of MicrobialNC observed in this study and in Zhou et al. (2023). The studies above demonstrate comprehensively that the rapid permafrost degradation in the Tibetan Plateau causes substantial losses in SOC. However, there exists remarkable heterogeneity in SOC component changes across different regions. This warrants further investigation into the patterns of soil carbon component changes induced by permafrost thermokarst landforms. It involves exploring the influencing factors and analyzing their impacts. Furthermore, both Zhou et al. (2023) and this study used the calculation method from Liang et al. (2019) when calculating MicrobialNC. However, since this method (Liang et al., 2019) was derived from global temperate agricultural, grassland, and forest ecosystems and did not include permafrost soils in its parameter calibration calculations, there is some limitation in the calculation of MicrobialNC in permafrost soils (meadow

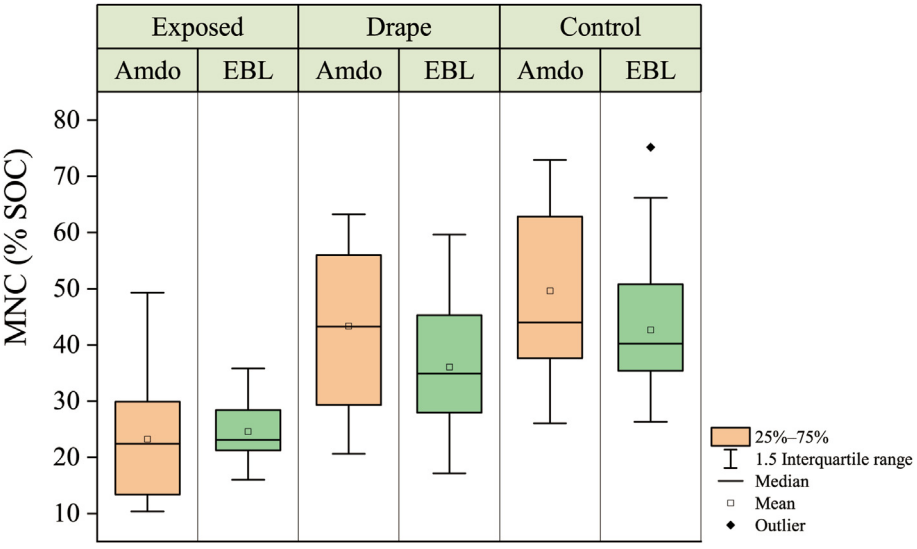

Fig. 7. Changes in microbial necromass carbon (MNC) at different sites in the central Tibetan Plateau (Amdo) and northern Tibetan Plateau (EBL, Zhou et al., 2023) during different stages (control, collapsing, and subsided) of permafrost thaw-subsidence.

Please cite this article as: ZHOU, W.-T., et al., Profound loss of microbial necromass carbon in permafrost thaw-subsidence in the central Tibetan Plateau, Advances in Climate Change Research, https://doi.org/10.1016/j.accre.2024.07.002

environments in this study). This requires further improvement in future research.

5. Conclusions

Dramatic permafrost degradation, such as thaw-subsidence, observed in the present study has shown significant alterations to the microenvironment, potentially leading to changes in the rates of carbon accumulation and decomposition from various sources. This study highlights the substantial loss of permafrost carbon in thaw-subsidence areas, primarily attributed to the decline of microbial necromass carbon. Our findings indicate that before the thaw-induced settlement, the permafrost had a SOC concentration of 72.68 ± 18.53 mg g^{-1}, with MicrobialNC accounting for 49.6%. It is found that 56.4% of SOC is lost in permafrost thaw-subsidence, with microbial necromass carbon accounting for around 70.0% of the carbon loss. The substantial reduction in microbial necromass carbon is correlated with variations in pH, plant input, and microbial properties in thaw-subsidence. The significant physicochemical protection observed in other studies is not reflected. Drawing from our investigation and prior research, the thawing of permafrost in the Tibetan Plateau leads to a considerable reduction in SOC. Nonetheless, notable diversity in SOC component alterations among distinct regions.

Declaration of competing interest

The authors declare no conflict of interest.

CRediT authorship contribution statement

Wenting Zhou: Writing − original draft, Visualization, Software, Methodology, Conceptualization. **Quanlian Li:** Writing − review & editing, Methodology. **Shichang Kang:** Writing − review & editing, Supervision, Conceptualization. **Xiaodong Wu:** Writing − review & editing, Supervision. **Tian Ma:** Writing − review & editing, Methodology. **Xiaobo Wu:** Writing − review & editing, Methodology. **Xin Xiong:** Writing − review & editing, Methodology. **Tanuj Shukla:** Writing − review & editing. **Maheswar Rupakheti:** Writing − review & editing. **Dipesh Rupakheti:** Writing − review & editing. **Dahe Qin:** Writing − review & editing, Supervision. **Xiufeng Yin:** Writing − original draft, Visualization, Methodology, Conceptualization.

Acknowledgments

This study was supported by the National Natural Science Foundation of China (U23A2062, 32361133551), State Key Laboratory of Cryospheric Science (SKLCS-ZZ-2023), Second Tibetan Plateau Scientific Expedition and Research Program (STEP, 2019QZKK0605), and Natural Science Foundation of Gansu Province (21JR7RA500 and 22ZD6FA005). We appreciate Linwei Lu's great help in the field work.

Appendix A. Supplementary data

Supplementary data to this article can be found online at https://doi.org/10.1016/j.accre.2024.07.002.

References

Appuhn, A., Joergensen, R.G., 2006. Microbial colonisation of roots as a function of plant species. Soil Biol. Biochem. 38, 1040−1051. https://doi.org/10.1016/j.soilbio.2005.09.002.

Bahram, M., Hildebrand, F., Forslund, S.K., et al., 2018. Structure and function of the global topsoil microbiome. Nature 560, 233−237. https://doi.org/10.1038/s41586-018-0386-6.

Bossio, D.A., Scow, K., 1998. Impacts of carbon and flooding on soil microbial communities: phospholipid fatty acid profiles and substrate utilization patterns. Microb. Ecol. 35, 265−278. https://doi.org/10.1007/s002489900082.

Brown, J., Romanovsky, V.E., 2008. Report from the international permafrost association: state of permafrost in the first decade of the 21st century. Permafr. Periglac. Process. 19, 255−260. https://doi.org/10.1002/ppp.618.

Cao, Y., Ding, J., Li, J., et al., 2023. Necromass-derived soil organic carbon and its drivers at the global scale. Soil Biol. Biochem. 181, 109025. https://doi.org/10.1016/j.soilbio.2023.109025.

Chang, R., Liu, S., Chen, L., et al., 2021. Soil organic carbon becomes newer under warming at a permafrost site on the Tibetan Plateau. Soil Biol. Biochem. 152, 108074. https://doi.org/10.1016/j.soilbio.2020.108074.

Chen, L., Liang, J., Qin, S., et al., 2016. Determinants of carbon release from the active layer and permafrost deposits on the Tibetan Plateau. Nat. Commun. 7, 13046. https://doi.org/10.1038/ncomms13046.

Chen, L., Liu, L., Mao, C., et al., 2018. Nitrogen availability regulates topsoil carbon dynamics after permafrost thaw by altering microbial metabolic efficiency. Nat. Commun. 9, 3951. https://doi.org/10.1038/s41467-018-06232-y.

Chen, L., Smith, P., Yang, Y., 2015. How has soil carbon stock changed over recent decades? Global Change Biol. 21, 3197−3199. https://doi.org/10.1111/gcb.12992.

Deng, F., Liang, C., 2022. Revisiting the quantitative contribution of microbial necromass to soil carbon pool: stoichiometric control by microbes and soil. Soil Biol. Biochem. 165, 108486. https://doi.org/10.1016/j.soilbio.2021.108486.

Frostegård, A., Bååth, E., 1996. The use of phospholipid fatty acid analysis to estimate bacterial and fungal biomass in soil. Biol. Fertil. Soils 22, 59−65. https://doi.org/10.1007/BF00384433.

Guckert, J.B., Antworth, C.P., Nichols, P.D., et al., 1985. Phospholipid, ester-linked fatty acid profiles as reproducible assays for changes in prokaryotic community structure of estuarine sediments. FEMS (Fed. Eur. Microbiol. Soc.) Microbiol. Ecol. 1, 147−158. https://doi.org/10.1111/j.1574-6968.1985.tb01143.x.

Guggenberger, G., Frey, S.D., Six, J., et al., 1999. Bacterial and fungal cell-wall residues in conventional and no-tillage agroecosystems. Soil Sci. Soc. Am. J. 63, 1188−1198. https://doi.org/10.2136/sssaj1999.6351188x.

Gupta, A., Gupta, R., Singh, R.L., 2017. Microbes and Environment. Principles and Applications of Environmental Biotechnology for a Sustainable Future. Springer Singapore, pp. 43−84. https://doi.org/10.1007/978-981-10-1866-4_3.

He, M., Fang, K., Chen, L., et al., 2022. Depth-dependent drivers of soil microbial necromass carbon across Tibetan alpine grasslands. Global Change Biol. 28, 936−949. https://doi.org/10.1111/gcb.15969.

Hemingway, J.D., Rothman, D.H., Grant, K.E., et al., 2019. Mineral protection regulates long-term global preservation of natural organic carbon. Nature 570, 228−231. https://doi.org/10.1038/s41586-019-1280-6.

Hu, Y., Zheng, Q., Noll, L., et al., 2020. Direct measurement of the in situ decomposition of microbial-derived soil organic matter. Soil Biol. Biochem. 141, 107660. https://doi.org/10.1016/j.soilbio.2019.107660.

IPCC, 2021. Climate Change 2021: The Physical Science Basis. Contribution of Working Group I to the Sixth Assessment Report of the

Intergovernmental Panel on Climate Change. Cambridge University Press, Cambridge and New York. http://hdl.handle.net/10204/12710.

Jensen, A., Lohse, K., Crosby, B., et al., 2014. Variations in soil carbon dioxide efflux across a thaw slump chronosequence in northwestern Alaska. Environ. Res. Lett. 9, 025001. https://doi.org/10.1088/1748-9326/9/2/025001.

Jones, D.L., Cooledge, E.C., Hoyle, F.C., et al., 2019. pH and exchangeable aluminum are major regulators of microbial energy flow and carbon use efficiency in soil microbial communities. Soil Biol. Biochem. 138, 107584. https://doi.org/10.1016/j.soilbio.2019.107584.

Kleber, M., Eusterhues, K., Keiluweit, M., et al., 2015. Mineral−organic associations: formation, properties, and relevance in soil environments. Adv. Agron. 130, 1−140. https://doi.org/10.1016/bs.agron.2014.10.005.

Lauer, F., Kösters, R., Du Preez, C.C., et al., 2011. Microbial residues as indicators of soil restoration in South African secondary pastures. Soil Biol. Biochem. 43, 787−794. https://doi.org/10.1016/j.soilbio.2010.12.012.

Li, J., Zhang, X., Luo, J., et al., 2020. Differential accumulation of microbial necromass and plant lignin in synthetic versus organic fertilizer-amended soil. Soil Biol. Biochem. 149, 107967. https://doi.org/10.1016/j.soilbio.2020.107967.

Li, N., Xu, Y., Han, X., et al., 2015. Fungi contribute more than bacteria to soil organic matter through necromass accumulation under different agricultural practices during the early pedogenesis of a Mollisol. Eur. J. Soil Biol. 67, 51−58. https://doi.org/10.1016/j.ejsobi.2015.02.002.

Liang, C., Amelung, W., Lehmann, J., et al., 2019. Quantitative assessment of microbial necromass contribution to soil organic matter. Global Change Biol. 25, 3578−3590. https://doi.org/10.1111/gcb.14781.

Lindgren, A., Hugelius, G., Kuhry, P., 2018. Extensive loss of past permafrost carbon but a net accumulation into present-day soils. Nature 560, 219−222. https://doi.org/10.1038/s41586-018-0371-0.

Liu, F., Qin, S., Fang, K., et al., 2022. Divergent changes in particulate and mineral-associated organic carbon upon permafrost thaw. Nat. Commun. 13, 5073. https://doi.org/10.1038/s41467-022-32681-7.

Luo, J., Niu, F., Lin, Z., et al., 2019. Recent acceleration of thaw slumping in permafrost terrain of Qinghai−Tibet Plateau: an example from the Beiluhe Region. Geomorphology 341, 79−85. https://doi.org/10.1016/j.geomorph.2019.05.020.

Lützow, M.v., Kögel-Knabner, I., Ekschmitt, K., et al., 2006. Stabilization of organic matter in temperate soils: mechanisms and their relevance under different soil conditions: a review. Eur. J. Soil Sci. 57, 426−445. https://doi.org/10.1111/j.1365-2389.2006.00809.x.

Ma, T., Zhu, S., Wang, Z., et al., 2018. Divergent accumulation of microbial necromass and plant lignin components in grassland soils. Nat. Commun. 9, 1−9. https://doi.org/10.1038/s41467-018-05891-1.

Mao, C., Kou, D., Wang, G., et al., 2019. Trajectory of topsoil nitrogen transformations along a thermo-erosion gully on the Tibetan Plateau. J. Geophys. Res. B. 124, 1342−1354. https://doi.org/10.1029/2018JG004805.

Matthews, H.D., Gillett, N.P., Stott, P.A., et al., 2009. The proportionality of global warming to cumulative carbon emissions. Nature 459, 829−832. https://doi.org/10.1038/nature08047.

McKeague, J., Day, J., 1966. Dithionite-and oxalate-extractable Fe and Al as aids in differentiating various classes of soils. Can. J. Soil Sci. 46, 13−22. https://doi.org/10.4141/cjss66-003.

Miner, K.R., Turetsky, M.R., Malina, E., et al., 2022. Permafrost carbon emissions in a changing Arctic. Nat. Rev. Earth Environ. 3, 55−67. https://doi.org/10.1038/s43017-021-00230-3.

Mu, C., Abbott, B.W., Norris, A.J., et al., 2020. The status and stability of permafrost carbon on the Tibetan Plateau. Earth Sci. Rev. 211, 103433. https://doi.org/10.1016/j.earscirev.2020.103433.

Mu, C., Zhang, T., Wu, Q., et al., 2015. Organic carbon pools in permafrost regions on the Qinghai−Xizang (Tibetan) Plateau. Cryosphere 9, 479−486. https://doi.org/10.5194/tc-9-479-2015.

Natali, S.M., Holdren, J.P., Rogers, B.M., et al., 2021. Permafrost carbon feedbacks threaten global climate goals. Proc. Natl. Acad. Sci. USA 118, e2100163118. https://doi.org/10.1073/pnas.2100163118.

Neher, D.A., 2010. Ecology of plant and free-living nematodes in natural and agricultural soil. Annu. Rev. Phytopathol. 48, 371−394. https://doi.org/10.1146/annurev-phyto-073009-114439.

Schuur, E.A., Abbott, B., 2011. High risk of permafrost thaw. Nature 480, 32−33. https://doi.org/10.1038/480032a.

Six, J., Frey, S., Thiet, R., et al., 2006. Bacterial and fungal contributions to carbon sequestration in agroecosystems. Soil Sci. Soc. Am. J. 70, 555−569. https://doi.org/10.2136/sssaj2004.0347.

Sylvia, D.M., Fuhrmann, J.J., Hartel, P.G., et al., 2005. Principles and Applications of Soil Microbiology. Pearson. https://doi.org/10.2134/jeq2005.0731dup.

Wang, B., An, S., Liang, C., et al., 2021. Microbial necromass as the source of soil organic carbon in global ecosystems. Soil Biol. Biochem. 162, 108422. https://doi.org/10.1016/j.soilbio.2021.108422.

Wang, G., Liu, G., Li, C., et al., 2012. The variability of soil thermal and hydrological dynamics with vegetation cover in a permafrost region. Agric. For. Meteorol. 162, 44−57. https://doi.org/10.1016/j.agrformet.2012.04.006.

Wang, T., Yang, D., Yang, Y., et al., 2020. Permafrost thawing puts the frozen carbon at risk over the Tibetan Plateau. Sci. Adv. 6, eaaz3513. https://doi.org/10.1126/sciadv.aaz3513.

Whalen, E.D., Grandy, A.S., Sokol, N.W., et al., 2022. Clarifying the evidence for microbial-and plant-derived soil organic matter, and the path toward a more quantitative understanding. Global Change Biol. 28, 7167−7185. https://doi.org/10.1111/gcb.16413.

Wu, X., Zhao, L., Liu, G., et al., 2018. Effects of permafrost thaw-subsidence on soil bacterial communities in the southern Qinghai−Tibetan Plateau. Appl. Soil Ecol. 128, 81−88. https://doi.org/10.1016/j.apsoil.2018.04.007.

Zelles, L., 1999. Fatty acid patterns of phospholipids and lipopolysaccharides in the characterisation of microbial communities in soil: a review. Biol. Fertil. Soils 29, 111−129. https://doi.org/10.1007/s003740050533.

Zhao, L., Hu, G., Wu, X., et al., 2021. Dynamics and characteristics of soil temperature and moisture of active layer in the central Tibetan Plateau. Geoderma 400, 115083. https://doi.org/10.1016/j.geoderma.2021.115083.

Zhou, W., Ma, T., Yin, X., et al., 2023. Dramatic carbon loss in a permafrost thaw slump in the Tibetan Plateau is dominated by the loss of microbial necromass carbon. Environ. Sci. Technol. 57, 6910−6921. https://doi.org/10.1021/acs.est.2c07274.

Zou, D., Zhao, L., Sheng, Y., et al., 2017. A new map of permafrost distribution on the Tibetan Plateau. Cryosphere 11, 2527−2542. https://doi.org/10.5194/tc-11-2527-2017.

Please cite this article as: ZHOU, W.-T., et al., Profound loss of microbial necromass carbon in permafrost thaw-subsidence in the central Tibetan Plateau, Advances in Climate Change Research, https://doi.org/10.1016/j.accre.2024.07.002